Clays and Clay Minerals (2024), **72**, e34, 1–10
doi:10.1017/cmn.2024.34

Original Paper

Development and characterization of organically grafted clay minerals for the removal of methylene blue from water

Aizhan M. Serikbayeva[1,2,3], Fernanda F. Roman[1,2], Helder T. Gomes[1,2] and Marzhan S. Kalmakhanova[3]

[1]Centro de Investigação de Montanha (CIMO), Instituto Politécnico de Bragança, Campus de Santa Apolónia, 5300-253 Bragança, Portugal; [2]Laboratório para a Sustentabilidade e Tecnologia em Regiões de Montanha (SusTEC), Instituto Politécnico de Bragança, Campus de Santa Apolónia, 5300-253 Bragança, Portugal and [3]M.Kh. Dulaty Taraz University, Department of Chemistry and Chemical Technology, Taraz 080012, Kazakhstan

Abstract

In recent years, water pollution caused by industrial waste has been a major problem throughout the world. To remove harmful impurities from water, using methylene blue (MB) as a model compound, modified clays were used, as they are capable of adsorbing various substances on their surfaces. The modified clays were obtained by grafting dimethyl sulfoxide (DMSO) and triethanolamine (TEOA) in the space between the layers of Shymkent clay. DMSO was first added to the natural clay; TEOA was also added at a temperature of 180°C and then held at that temperature for 2 h. The resulting modified clays were dried at 60°C for 24 h and characterized by X-ray diffraction (XRD), surface area analysis (SAA), Fourier-transform infrared spectroscopy (FT-IR), elemental analysis, and thermogravimetric analysis (DTA and TGA). Natural and modified clays (0.25–2.5 g L^{-1}, pH=1–12, and 50°C) were used to adsorb MB from an aqueous solution at a concentration of 50 mg L^{-1}. Contact with the adsorbent was maintained for 8 h. As much as 95.9% of the MB was removed from the aqueous solution in as little time as 15 min. Adsorption conditions were optimized, and the clay modified with TEAO showed better results than the natural clay (85% for modified clay *vs* 40% for original clay, at a clay concentration of 0.5 g L^{-1}); significant adsorption was obtained over a wide pH range (>85% from pH 1 to 12).

Keywords: adsorption; dimethyl sulfoxide; methylene blue; organoclays; triethanolamine

(Received: 03 January 2024; revised: 09 October 2024; accepted: 18 October 2024)

Introduction

Organic dyes represent a large group of pollutants in wastewaters of textile, paper, plastic, food, and other industries. With the production of 70,000 tons of ~10,000 types of dyes and pigments worldwide annually, about 1–15% of dyes are estimated to be lost as wastes during dyeing processes (Elmoubarki et al., 2015). Organic dyes, especially cationic dyes, are used widely due to their ease of application and durability, but the side-effects are significant. Cationic dyes are recognized as carcinogenic and mutagenic, and have a strong staining effect on the entire ecosystem when disposed as waste into the environment, even at low concentrations (Tkaczyk et al., 2020). Therefore, reducing the concentration of dyes in wastewaters before discharge into the environment is important and the development of appropriate purification processes is essential (Tripathi et al., 2023). Methylene blue (MB) is a cationic dye that has a very wide application and is becoming one of the most common colored pollutants in waters. Among several chemical and physical methods of wastewater treatment, adsorption is an effective and efficient method for removing dyes, using various clay-based adsorbents such as bentonite (Jawad et al., 2023), Moroccan clay (Souhassou et al., 2023), montmorillonite (Mundkur et al., 2022), and others. In general, raw kaolin-based clays (Koteja and Matusik, 2015) are not suitable adsorbents due to the limited specific surface area and low layer charge, which limit the extent of ion-exchange processes on their surfaces. Nevertheless, studies have shown that kaolin-based clay minerals can be modified to become better adsorbers by intercalating or grafting organic compounds into the interlayer space, leading to hybrid organic-mineral materials with suitable properties for adsorption and several other applications (Koteja and Matusik, 2015; Mukhopadhyay et al., 2021). Other modifications have been reported to increase the adsorption capacity of kaolin-based clays, such as pillaring (Mnasri-Ghnimi and Frini-Srasra, 2019; Silva et al., 2019; Reimbaeva et al., 2020; Zhang et al., 2021), acid activation (Silva et al., 2019; Zhang et al., 2021), and magnetic activation (Ahmadi et al., 2020; Esvandi et al., 2020; Baimuratova et al., 2022; Baimuratova et al., 2024); but, to the best of the present authors' knowledge, organic grafting remains largely unexplored for adsorption processes, especially for MB adsorption (see Fig. S1a in the Supplementary material). Clays with embedded organic compounds are expected to provide a better adsorption capacity for dyes (Haleem et al., 2023). In particular, amines, such as triethanolamine (TEAO), act as

Corresponding author: Marzhan S. Kalmakhanova; marjanseitovna@mail.ru
Cite this article: Serikbayeva A.M., Roman F.F., Gomes H.T., & Kalmakhanova M.S. (2024). Development and characterization of organically grafted clay minerals for the removal of methylene blue from water. *Clays and Clay Minerals* **72**, e34, 1–10. https://doi.org/10.1017/cmn.2024.34

Lewis bases (Zakharova et al., 2018) and, thus, increase the number of active centers for the adsorption of cationic dyes (Yang et al., 2019), such as MB, over a wide pH range.

Clays belonging to the kaolin group (1:1 layers) characteristically have a smaller cation exchange capacity and surface area than many 2:1 layered minerals, such as smectite (Qi et al., 2023), and thus are only good for adsorption purposes if their layers are opened by means of intercalation. Only a few molecules can be intercalated into the 1:1 layer (Lagaly et al., 2013). As a result, they are not as widely modified by organic grafting as 2:1 layered clays (such as bentonites and montmorillonite; see Fig. S1b in the Supplementary material). Furthermore, few studies exist in the literature with kaolinite clays used for the adsorption of dyes with organoclays (Ferreira et al., 2017). To the best of the present authors' knowledge, the application of kaolinite clays modified with TEAO in the adsorption of MB, reported here, has not been tested previously. Because direct intercalation of bulky compounds (such as TEAO) into the interlayer space of kaolinite is not feasible (Letaief and Detellier, 2011), due to strong interactions between the tetrahedral and the octahedral sheets of the clay, the smaller dipolar dimethyl sulfoxide (DMSO) was pre-intercalated (yielding Shymkent-DMSO) and used as the precursor for further intercalation of TEAO. In this process, TEAO is inserted into the interlayer spaces of kaolinite upon displacement of DMSO, yielding stable kaolinite organo-grafted clays resulting from the formation of a covalent bond between the hydroxyl groups of TEAO and the aluminol groups of the internal surfaces of kaolinite. Both raw and modified clays were tested in the adsorption of MB, and adsorption conditions were evaluated using the Shymkent-TEAO sample. The amine center introduced in the sample allowed fast MB adsorption over a wide pH range, supporting the hypothesis that was tested regarding the development of highly adsorptive kaolinite organo-grafted clays with TEAO.

Materials and methods

Materials and reactants

In the present study, a natural kaolinite clay was obtained from a deposit found at Shymkent, Kazakhstan, and is referred here as Shymkent clay. Dimethyl sulfoxide (DMSO, C_2H_6OS, 99.5%) was supplied by Stanlab PURE, dioxane ($C_4H_4O_2$, 99.5%) was supplied by DiAKiT, isopropanol (C_3H_8O, 99.7%) was supplied by LaborPharm (Astana, Kazakhstan), triethanolamine (TEAO, $C_6H_{15}NO_3$, 95%) was supplied by Tomas.kz. Methylene blue (98%) was supplied by Merck. All reactants were used without modification. Distilled water (resistivity of 18.2 Mohm-cm) was used throughout.

Synthesis of organo-modified clay materials

For the manufacture of materials with adsorption properties, the natural clay was first ground to powder in a mill and passed through a sieve with 0.063 mm maximum particle size. To modify the natural clay, 6 g of the clay was initially suspended in 6 L of water and then added to a mixture containing 30 mL of DMSO and 2.5 mL of water. The suspension was kept under magnetic stirring at a temperature of 80°C for 5 days, and then the mixture was left at room temperature for 2.5 days. The resulting material was extracted after two series of centrifugation using, first, dioxane (2×25 mL), and then isopropanol (2×25 mL). The product was dried at 50°C, leading to the modified clay Shymkent-DMSO. Shymkent-DMSO clay was further grafted with TEAO, generating a modified Shymkent-TEAO sample. One gram of Shymkent-DMSO was added to 6 g of TEOA and stirred at 180°C for 2 h, and then washed with isopropanol (3×50 mL). The resulting material was dried at 50°C for 24 h, leading to Shymkent-TEAO.

Characterization of the materials

Thermogravimetric analyses were performed using a Derivatograph device (MOM, Budapest, Hungary). The method used is based on recording changes in the thermochemical and physical parameters of a substance that are caused when that substance is heated. The thermochemical state of the sample is described by the *T* (temperature), DTA (differential thermal analysis), TG (thermogravimetric analysis), and DTG (differential thermogravimetric analysis) curves, the last of these being a derivative of the TG function. The materials did not undergo any specific treatment for the TGA analysis, and the analysis of the materials was carried out in air atmosphere, in the temperature range from 20 to 1000°C at a heating rate of 10°C min^{-1}.

The textural properties of the materials were determined by analysis of N_2 adsorption–desorption isotherms at –196°C, obtained using a Quantachrome NOVAtouch XL4 adsorption analyzer following procedures reported elsewhere (Diaz de Tuesta et al., 2018; Karimi et al., 2020; Diaz de Tuesta et al., 2021). All calculations were carried out using the software *Quantachrome TouchWin*™ v1.21. Prior to analysis, the materials were degassed at 120°C for 16 h. The surface areas (S_{BET} and $S_{Langmuir}$) were determined using the methods of BET and Langmuir with P/P_0 in the range 0.05–0.35. The external surface area (S_{ext}) and micropore volume (V_{mic}) were obtained by the t-plot method (thickness was calculated using the ASTM standard D-6556-1). The micropore surface area, S_{mic}, was determined by the subtraction of S_{EXT} and S_{BET}, and the pore width (W_{mic}) was obtained by approximation ($W_{mic} = 4–V_{mic}/S_{mic}$). The equations used for determining $S_{Langmuir}$ and S_{BET} are described in the Supplementary material (see also Lowell et al., 2004; Bardestani et al., 2019; Diaz de Tuesta et al., 2022). The total pore volume (V_{total}) was determined at P/P_0=0.98. Studies of the morphology of the samples were carried out using a scanning electron microscope (SEM) JEOL JSM-6490LV with INCA Energy Microanalysis and HKL basic structural analysis systems. The multi-purpose SEM (useful magnification of 300,000×) combined the possibilities of working in both standard and low-vacuum modes, allowing the direct examination of samples in powder form without spraying with a conductive layer.

The pH of the point of zero charge (pH_{pzc}) was determined using pH drift tests, adapting the procedure described by Silva et al. (2019). In short, five solutions of NaCl (0.01 M) were prepared as electrolyte with a variable initial pH (in the range of 1–12, using HCl and NaOH 0.1 M solutions). Clay sample (0.05 g) in powder form was combined with 20 mL of each NaCl solution. The equilibrium pH of each suspension was measured after 48 h under stirring (320 rpm) at room temperature. The pH_{pzc} value was determined by crossing the curve 'final pH *vs* initial pH' with the straight line 'final pH = initial pH'.

The X-ray diffraction (XRD) patterns were acquired using an automated diffractometer DRON-3 instrument with SiKα radiation and a β filter. X-ray phase analysis on a semi-quantitative basis was performed using XRD patterns of powder samples. The materials did not undergo any specific treatment before the analysis. The quantitative ratios of the crystal phases were determined. The interpretation of patterns was carried out using data from

https://doi.org/10.1017/cmn.2024.34 Published online by Cambridge University Press

Table 1. Thermogravimetric data for the natural clay and of Shymkent-TEAO clay, in the temperature range 20–1000°C

Material	Weight-loss sequence	Weight loss (%)	Volatile components	Temperature range (°C)
Shymkent natural clay	Δm1	2.0	H_2O	20–200
	Δm2	0.875	OH	200–400
	Δm3	7.38	CO_2	400–725
	Δm4	0.125	OH	725–1000
	∑Δm1000°C	10.38	H_2O, OH, CO_2	20–1000
Shymkent-TEAO	Δm1	1.7	H_2O	20–200
	Δm2	1.4	OH	200–300
	Δm3	2.1(OH)+0.4(CO_2)	CO	300–~500
	Δm4	8.25	OH	500–720
	Δm5	1.0	OH	720–1000
	∑Δm1000°C	14.85	H_2O, OH	20–1000

the ICDD card file: PDF2 powder diffraction database (Powder Diffraction File) and patterns for minerals free of impurities. The DRON-3 diffractometer tube settings were 35 kV and 20 mA. Fourier-transform infrared (FT-IR) spectra were acquired using a Perkin Elmer UATR 2 FT-IR spectrophotometer at a resolution of 1 cm^{-1} and scan range of 4000 to 450 cm^{-1}. Prior to analysis, the materials were dried carefully at 105°C overnight. The materials (~1 mg) were previously mixed with KBr (~100 mg), crushed and pressed into a pellet using a manual hydraulic press (GS15011, Specac, UK) applying 10 tons of pressure.

Adsorption process and analytical methods

The MB adsorption tests were carried out by adding 0.125 g of adsorbent (natural and modified clays) to 50 mL of a 50 mg L^{-1} MB solution with a total contact time of 8 h at a temperature of 50°C. Sampling was undertaken at pre-determined intervals (0, 15, 30, 60, 120, 240, 360, or 480 min). The effects of various pH values of MB solution were tested (pH 1, 3, 6, 9, and 12). The adsorption tests also considered variations in the concentration of adsorbent (2.5, 0.5, and 0.25 g L^{-1}) and variations in the concentration of MB solution (50, 100, and 500 mg L^{-1}). The adsorption of MB was monitored at 664 nm using a UV-Vis spectrophotometer.

Results and Discussion

Thermal analysis (DTA and TGA)

As a result of the dynamic heating of these samples, the DTA, DTG, and TG curves revealed various types of reactions in the system (see Fig. S2 in the Supplementary material). Among them were the processes associated with the release of H_2O and hydroxyls into the atmosphere during the decomposition of clay minerals and reactions with CO_2 emissions because of the combustion of organic matter, as well as during the destruction of calcite. During the thermal decomposition of its mineral components, two pronounced effects were recorded, associated with the decomposition of gibbsite ($Al(OH)_3$) (in the range 20–200°C) and with the dissociation of calcium carbonate (in the range 400–725°C) (Fig. S2a).

Several thermal effects, mainly endothermic reactions, were observed in the heating curves of modified Shymkent-TEAO clay samples (Fig. S2b). The reactions that caused these manifestations were accompanied by the evolution of molecular water (Δm1 (1.7%), see Table 1 for definitions), hydroxyls (Δm2 (1.4%), Δm5 (1.0%)), carbon dioxide from the decomposition of calcite, as well as a result of joint losses (Δm3 (2.5%) = OH (2.2%) + CO_2 (0.3%)) at the destruction of kaolinite and combustion of S, respectively, as revealed by the reported semi-quantitative analysis (Table 1).

According to the thermogravimetric curve, in the first case, gibbsite was dehydrated (in two stages) with a weight loss equal to Δm1 – 0.3% = 1.7%, which corresponded to the presence of 8.1% of gibbsite in the Shymkent modified clay under dynamic heating from 20 to 1000°C, leaving a series of endothermic manifestations on the DTA curve at 190, 260, and ~500°C and one exothermic inflection point in the 900°C region. These endothermic reactions also took shape on the DTG curve in the form of clearly defined inflection points in the same temperature regions. Such processes were caused by thermal dehydration of minerals that were part of the test sample. At these temperatures, each such discharge from the water system left a corresponding step of weight loss on the thermogravimetric (TG) curve (Table 1). According to the atlas of thermal curves of minerals and rocks (Lorentz et al., 2018), the endothermic mass loss centered at 260°C was caused by the decomposition of gibbsite. The dehydration of this mineral, due to defects in its structure, proceeded in two stages. The total weight loss in this case reached the value of Δm1 + Δm2 = 8.58%, which corresponded to 13.1% of gibbsite in the sample. Along with this mineral, kaolinite was present in the sample; this was determined using the above-mentioned characteristics, viz. the endothermic effect at 500°C and the exothermic peak at 900°C (Khan et al., 2017). The effect found in the 500°C region was caused by dehydroxylation of the kaolinite structure.

When heated, kaolinite left on the DTA curve a weak peak in the range of 300–500°C and an equally weak feature in the region of 900°C. Thermal dissociation of this mineral occurred together with the combustion of organic matter. At the same time, kaolinite registered a weight loss from the modified Shymkent-TEAO clay of 2.2% (OH↑), and of organic matter of 0.3% (CO_2↑). Thus, the amount of this clay mineral corresponded to 8.3%, and the amount of organic matter in the sample, in accordance with the emissions from the CO_2 system, was 0.3% of the mass of the modified Shymkent-TEAO clay. Calcite showed itself most clearly during heating, leaving clearly defined events on the DTA and DTG curves

https://doi.org/10.1017/cmn.2024.34 Published online by Cambridge University Press

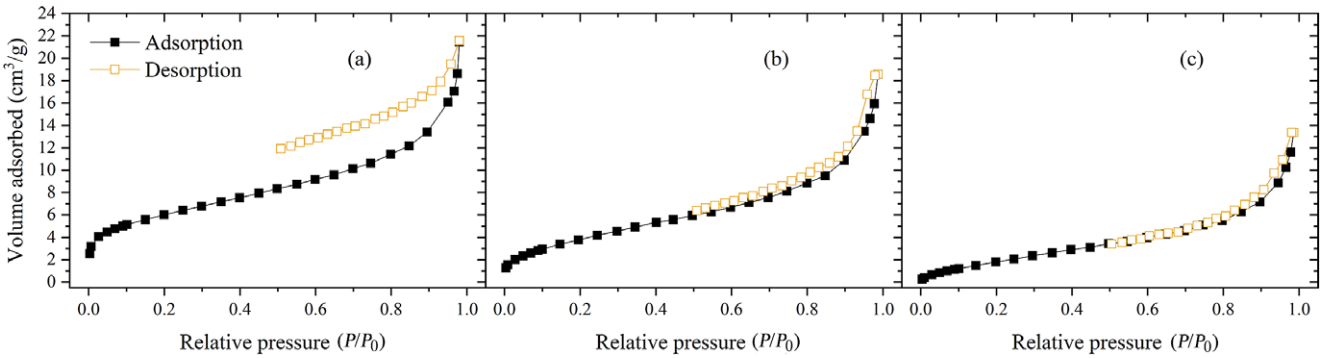

Figure 1. N_2 adsorption-desorption isotherms at –196°C of the (a) Shymkent natural clay, (b) Shymkent-DMSO, and (c) Shymkent-TEAO.

Table 2. Textural properties of the materials

Sample	S_{BET} (m^2 g^{-1})	$S_{Langmuir}$ (m^2 g^{-1})	S_{ext} (m^2 g^{-1})	V_{mic} (cm^3 g^{-1})	V_{total} (cm^3 g^{-1})	S_{mic} (m^2 g^{-1})	W_{mic} (nm)
Shymkent natural clay	21	25	13	0.00398	0.0288	8	1.9
Shymkent-DMSO	15	16	12	0.001025	0.0247	3	1.4
Shymkent-TEAO	9	8	9	0	0.0180	0	—

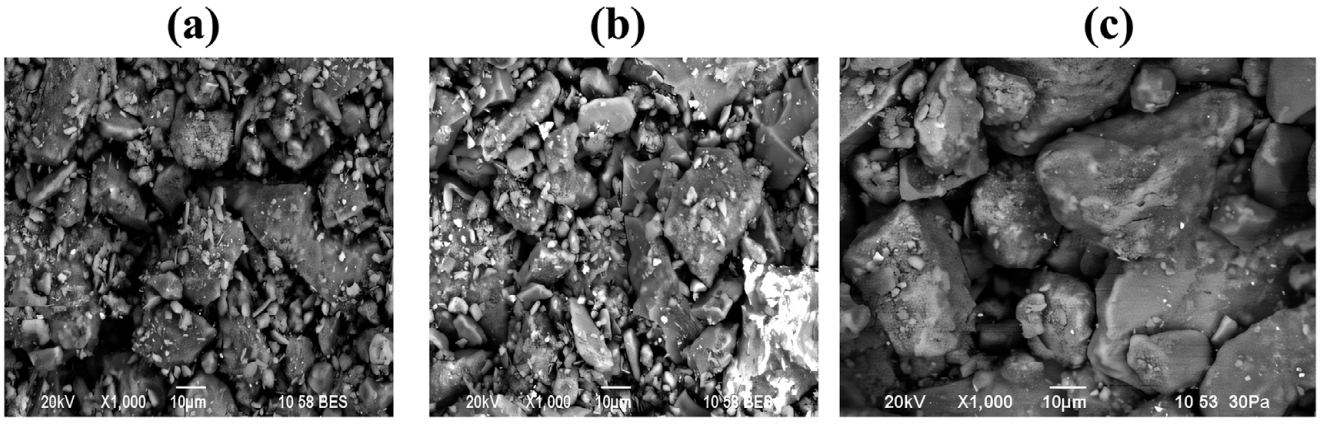

Figure 2. SEM images of: (a) Shymkent natural clay, (b) Shymkent-DMSO, and (c) Shymkent-TEAO.

in the region of 700°C due to carbon dioxide emissions into the atmosphere. At the same time, the weight loss of the modified Shymkent-TEAO clay was 8.25%, which corresponded to 18.8% of calcium carbonate in its composition (Yuan et al., 2008).

N_2 adsorption–desorption isotherms at 196°C

The N_2 adsorption–desorption isotherms of the adsorbents (Shymkent natural and modified clays) (Fig. 1) and the corresponding textural properties (Table 2) revealed isotherm patterns identified as type IV (Brunauer et al., 1940) with a type H3 hysteresis loop (Gregg and Sing, 1982), in accordance with the IUPAC classification. Type IV showed that the material had a mesoporous character, and the type H3 hysteresis loop showed the characteristics of a layered material with gaps similar to the pores formed by a plate layer with a space between arrays of plates (Sing et al., 1985; Auerbach et al., 2004). This also implied that DMSO and TEAO could maintain the area between the clay layers to remain supported to create a wider gallery.

The surface area decreased upon modification, which may indicate that DMSO and TEAO block the clay pores, especially the micropores (S_{mic}), with TEAO completely blocking access to the microporosity of the natural clay. Similar behavior was reported previously, with a S_{BET} decrease from 25 to 4 m^2 g^{-1} for montmorillonite-derived materials (Godarziani et al., 2022), and from 97 to 37–66 m^2 g^{-1} (Elkhalifah et al., 2014a; Elkhalifah et al., 2014b) for bentonite-derived materials when modified with TEAO. The micropore area has also been reported to decrease upon intercalation of TEAO (Godarziani et al., 2022).

Scanning electron microscopy

SEM images showed different morphologies for the Shymkent natural clay and the modified Shymkent-DMSO and Shymkent-TEAO clays (Fig. 2). The SEM images showed that the surface morphology of the Shymkent natural clay was typical of kaolinite (Cheng et al., 2010; Guerra et al., 2008; Sun et al., 2011; Caglar, 2012; Machado et al., 2012). The Shymkent clays modified with DMSO

https://doi.org/10.1017/cmn.2024.34 Published online by Cambridge University Press

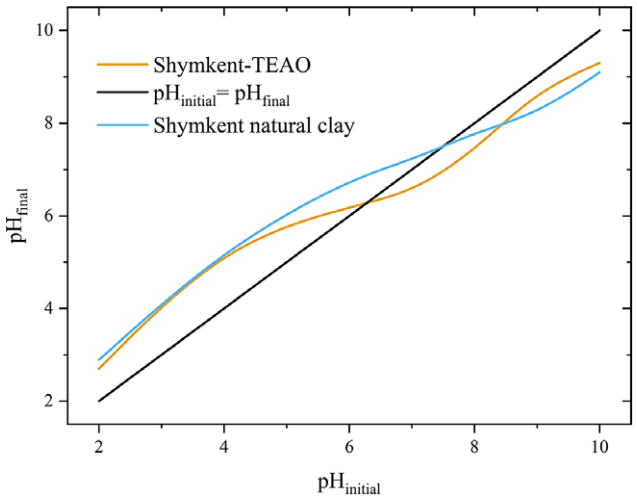

Figure 3. Determination of the pH_{pzc} values of the Shymkent natural clay and Shymkent-TEAO.

Table 3. Results of semi-quantitative X-ray phase analysis of crystal phases

Mineral	Formula	Shymkent (%)
Quartz	SiO_2	54.2
Kaolinite	$Al_2(Si_2O_5)(OH)_4$	10.6
Chlorite	$(Mg,Fe)_5Al(Si_3Al)O_{10}(OH)_8$	3.6
Mica	$KAl_2(AlSi_3O_{10})(OH)_2$	2.5
Feldspars (albite)	$Na(AlSi_3O_8)$	4.8
Calcite	$Ca(CO_3)$	13.3
Aluminum-potassium trisilicate	$KAlSi_3O_8$	4.0
Gypsum	$Ca(SO_4)(H_2O)_2$	3.1
Tremolite	$(Ca, Na, Fe)_2$ $Mg_5Si_8O_{22}(OH)_2$	3.8
Gibbsite	$Al(OH)_3$	—
Anatase	$Ti0.784O_2$	—
Rutile	TiO_2	—
Titanium silicate Silicalite	TiO_2–SiO_2	—
Analcime	$Na(AlSi_2O_6)(H_2O)$	—

and TEOA retained this aspect, but the size of the kaolinite particles was smaller due to intercalation of TEAO molecules (Guerra et al., 2008; Kausar and Bhatti, 2013). The modified clays had more spongy particles because of changes to the surface charge of the particle and the time spent preparing it (Caglar, 2012; Machado et al., 2012).

The pH of point of zero charge (pH_{pzc})

Procedures used to modify the corresponding pH_{pzc} value (Fig. 3) showed that the starting material (Shymkent natural clay) had a slightly basic character (pH_{pzc}=7.45). Upon modification with TEAO, the pH_{pzc} decreased and became slightly acidic (pH_{pzc}=6.25). Accordingly, the surface at pH<pH_{pzc} was positively charged. The value of pH_{pzc} depended directly on the amount of DMSO and TEAO introduced into the clay materials (Sing et al., 1985).

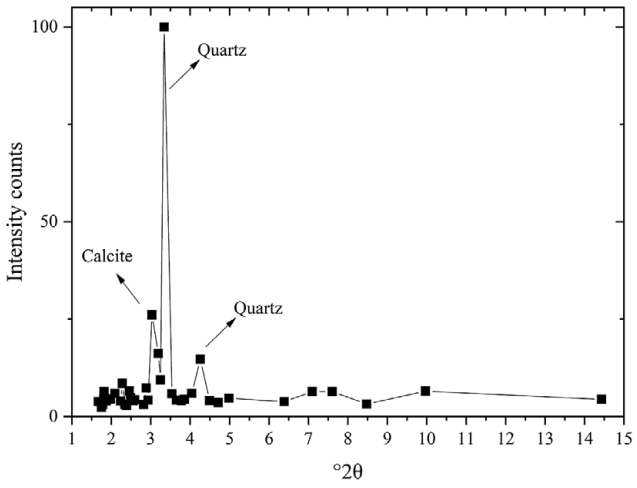

Figure 4. XRD pattern of the Shymkent natural clay.

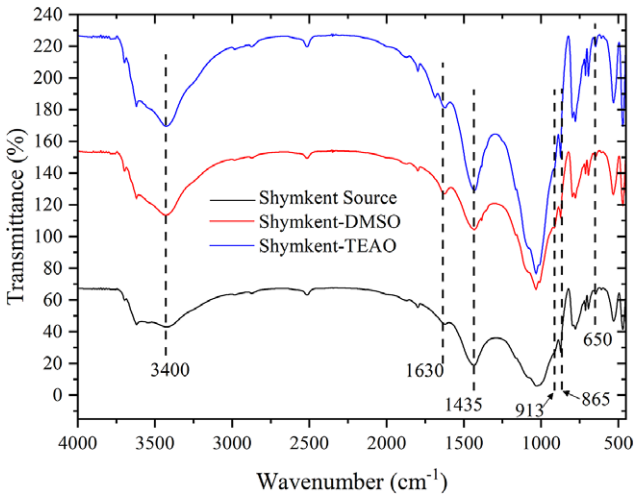

Figure 5. FT-IR spectra of the Shymkent natural clay, and of versions modified with DMSO and TEAO.

X-ray diffraction analysis

To determine the quantitative ratio of the crystalline phases of alumina in the natural clay from Shymkent, the samples were subjected to analysis by XRD (Table 3; Fig. 4). The results of the analysis established that the Shymkent clay consisted of layered silicates, primarily kaolinite $Al_2(Si_2O_5)(OH)_4$, quartz, and calcite, with a small amount of chlorite $(Mg,Fe)_5Al(Si_3Al)O_{10}(OH)_8$ and admixtures of muscovite $KAl_2(AlSi_3O_{10})(OH)_2$, albite $Na(AlSi_3O_8)$, $Ca(SO_4)(H_2O)_2$, $KAlSi_3O_8$, and tremolite $(Ca,Na,Fe)_2Mg_5Si_8O_{22}(OH)_2$. Other impurities may be present in small concentrations but were not identified unambiguously due to low-intensity reflections and/or poor crystallization (Serikbayeva et al., 2021).

Fourier-transform infrared spectroscopy

The FT-IR spectra of the clays (Fig. 5) revealed characteristic vibrations for tetrahedral Si-O-Si in the region 950–1250 cm^{-1} and octahedral Al-Al-OH at 913 cm^{-1}, Al-Fe-OH at 865 cm^{-1},

https://doi.org/10.1017/cmn.2024.34 Published online by Cambridge University Press

and for Mg-Mg-OH at 650 cm^{-1} (Ahmed et al., 2018). Furthermore, bands due to hydroxyls and water molecules were observed at ~3200–3400 and 1435 cm^{-1}, respectively. The interactions between organic molecules and silicates were observed in the region 1200–2000 cm^{-1} (Junior et al., 2020). The typical bands of amine groups were observed at 1630 cm^{-1}, confirming the grafting. The intensities of the bands in the high-wavenumber region decreased as a result of the condensation of silanes with Mg-OH or Al-OH groups from the fibrous structures. In addition, new bands at 3479 and 3410 cm^{-1} were ascribed to amino groups. The absorption band at 2930 cm^{-1} corresponded to the C–H stretching vibration of CH_2 groups (Ahmed et al., 2018).

The FT-IR spectra of the natural clays (Fig. 5) contained characteristic peaks for kaolinite and showed evidence of intercalation and grafting of DMSO and TEAO. The kaolinite band at 850 cm^{-1}, attributed to the vibration of hydroxyl groups of the inner surface during smooth bending was sensitive to intercalation and grafting, the band shifting to 726 cm^{-1}. In addition, intercalation of TEAO led to a significant decrease in the intensity of the hydroxyl band of the inner surface at 3600 cm^{-1} and to the appearance of a new peak at 3044 cm^{-1} (Fig. 5; DMSO and TEAO). The peak is formed as a result of an H bond between TEAO and hydroxyl groups of the clay inner surface at 1798 cm^{-1}. The stretching peak of Shymkent-TEAO at 1792 cm^{-1} changed to 1549 cm^{-1} for the Shymkent-DMSO, indicating that the DMSO molecule forms an H bond with hydroxyls through carbonyl oxygen. In addition, the stretching peak of Shymkent-TEAO at 1310 cm^{-1} was observed at 1385 cm^{-1} for Shymkent-DMSO. In addition, the N–H deformation peaks of Shymkent-TEAO were shifted from 1549 cm^{-1} to 1377 cm^{-1}, and the peaks of C–H stretching of Shymkent-TEAO are shifted from 2968, 2937, and 2798 cm^{-1}, to 2968, 2937, and 2576 cm^{-1}, respectively.

Adsorption of methylene blue

Effect of modification

Methylene blue was adsorbed by the Shymkent natural clay, Shymkent-DMSO, and Shymkent-TEAO (Fig. 6), using a dosage of 50 mg MB and 2.5 g of adsorbent. Similar results were found for each adsorbent in which nearly complete removal of MB was achieved after only 15 min. Very little additional adsorption occurred after even 480 min. Studies were then carried out to determine the optimum MB to adsorbent ratio.

Effect of adsorbent dosage

The adsorbent dosage was varied from 0.25 to 0.5 g per 50 mg of MB considering both the natural and TEAO-modified Shymkent clay (Fig. 7). When using the Shymkent natural clay at an adsorbent dosage of 2.5 g per 50 mg of MB, the adsorption, as previously reported (Fig. 6), was very quick: within the first 15 min of contact time, all MB had been adsorbed. By reducing the dosage to 0.5 g per 50 mg of MB, this behavior changed drastically: within the first 45 min of contact time, scarcely 35% of the MB was removed, whereas at an adsorbent dosage of 0.25 g per 50 mg of MB the removal rate was ~20%. When using Shymkent-TEAO at the dosage levels of 0.5 and 0.25 g per 50 mg of MB, a sharp improvement compared with the natural clay was observed. After 480 min of contact time, both dosages led to removals of >86% of the original concentration of MB (which is equivalent to an adsorbed quantity of Q=159 mg g^{-1}, calculated according to Saeed et al., 2020). The greater degree of adsorption by the modified clay was in the range of 1.10–4.80×, depending on the adsorbent concentration and

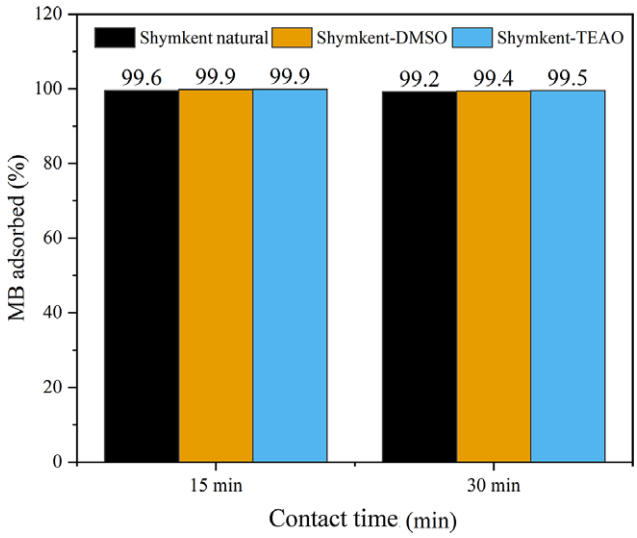

Figure 6. Effect of clay modification on adsorption of methylene blue. Conditions: $[MB]_0$=50 mg L^{-1}, $C_{adsorbent}$=2.5 g L^{-1}, T=50°C, pH_0=3.0.

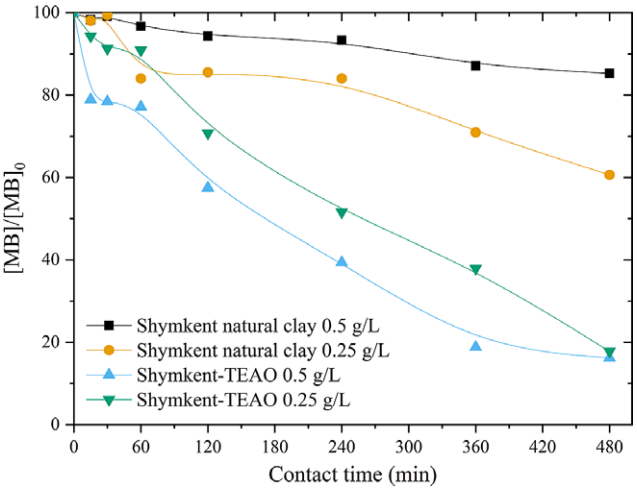

Figure 7. Effect of adsorbent concentration on methylene blue adsorption by Shymkent and Shymkent-TEAO. Conditions: $[MB]_0$=50 mg L^{-1}; $C_{adsorbent}$=0.25 and 0.5 g L^{-1}; T=50°C; pH_0=3.0.

contact time. Similar observations have been reported previously, with increases in the adsorption capacity of TEAO-modified kaolinites in the range of 1.25–2.5× greater than the raw clay (Koteja and Matusik, 2015) and 5–20× greater for halloysite-modified clay (Matusik and Wścisło, 2014) for adsorption of various heavy metals. Adsorption is a process that is not only governed by surface area, but the surface chemistry plays a significant role in adsorption process (Ruiz-Rosas et al., 2019; Kalmakhanova et al., 2023). In the case of the present study, given that the surface area was small even before organic grafting, surface area was not the key parameter driving adsorption. TEAO is a molecule containing nitrogenated moieties, which can behave as a Lewis base (Matusik and Wścisło, 2014) and allow interaction with MB. The increase in adsorbent also resulted in increased adsorption. For natural clay, this increase was in the range of 1.10–1.40× for an adsorbent concentration of 0.5 g per 50 mg of MB compared with 0.25 g per 50 mg of MB, depending on contact time. For Shymkent-TEAO this difference was in the range of 1.15–1.30×. Thus, for this

https://doi.org/10.1017/cmn.2024.34 Published online by Cambridge University Press

range of low adsorbent doses, the effect of modifying the clay is much more pronounced than the adsorbent concentration, allowing for a more sustainable and economic implementation of the process. The adsorption of a range of dyes by organoclays, as described in the literature, is noted in Table S1 (Suchithra et al., 2012; Fan et al., 2014; Ferreira et al., 2017; Ali et al., 2020; Rahmani et al., 2020; Saeed et al., 2020; Teixeira et al., 2023). As observed, the results reported here compare well with previous reports in the literature, surpassing them in some cases. Note that commercially or industrially available clays that often are used may be purer than the natural clays used in the present study.

Effect of pH

The effect of the solution pH may play an important role in the adsorption process, as this parameter changes the chemical composition of the dye solution and the charge of the functional groups of the adsorbents (Nadeem et al., 2016). The effect of pH was studied (Fig. 8). Usually, at a low pH, the removal percentage of an anionic dye from the solution would increase due to the electrostatic attraction between the positive surface charge of the adsorbent and the anionic dye. On the other hand, an electrostatic attraction between a negatively charged adsorbent and a positively charged dye molecule would occur if the solution had a high pH (basic), which would lead to a decrease in the percentage of anionic dye removal (Rashid et al., 2016; Tahir et al., 2016a; Naeem et al., 2017; Shoukat et al., 2017). At high pH, the adsorption capacity and removal of cationic dyes should increase, as the positive charges in the dye should ensure their attraction by the anionic adsorbent; an electrostatic attraction would thus occur between the positive charges of the dye and the negative surface of the adsorbent (Sharma 2015; Tahir et al., 2016b; Tahir et al., 2017). However, a decrease was observed in the ability of Shymkent-TEAO clay to adsorb MB with an increase in the pH of the initial suspension (Fig. 8). The adsorption of the cationic molecule of MB should be greater at higher pH, but, as seen in Fig. 8, there is no significant effect of pH. The maximum MB removal was observed at pH=3.0, where the modified clay removed up to 98% of MB. Given the pH_{pzc} of Shymkent-TEAO (pH_{pzc}=6.25) (Fig. 3), an excess of cations (H^+) at the surface of the adsorbents was expected. However, as previously discussed, the nitrogenated moiety from the TEAO molecule behaves as a Lewis base, being negatively charged (Matusik and Wścisło, 2014); thus, it allowed sufficient interaction between the adsorbent surface and the MB. The Shymkent-TEAO demonstrated flexibility, allowing its use over a wide range of pH values.

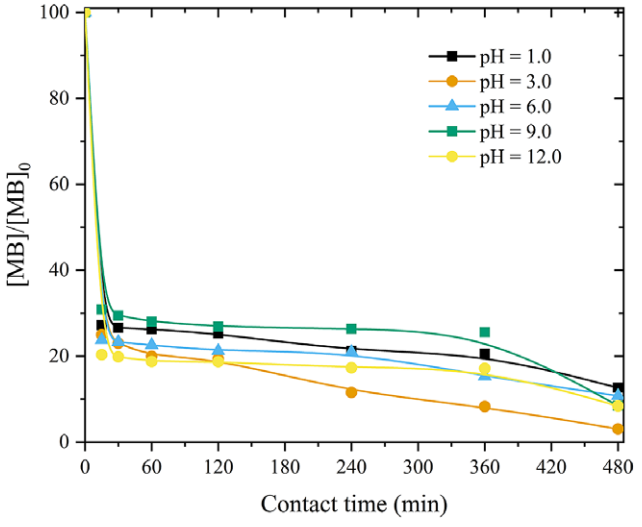

Figure 8. Effect of pH on adsorption of methylene blue by Shymkent-TEAO. Conditions: $[MB]_0$=50 mg L^{-1}; $C_{adsorbent}$=2.5 g L^{-1}; T=50°C; pH_0=1.0, 3.0, 6.0, 9.0, and 12.0.

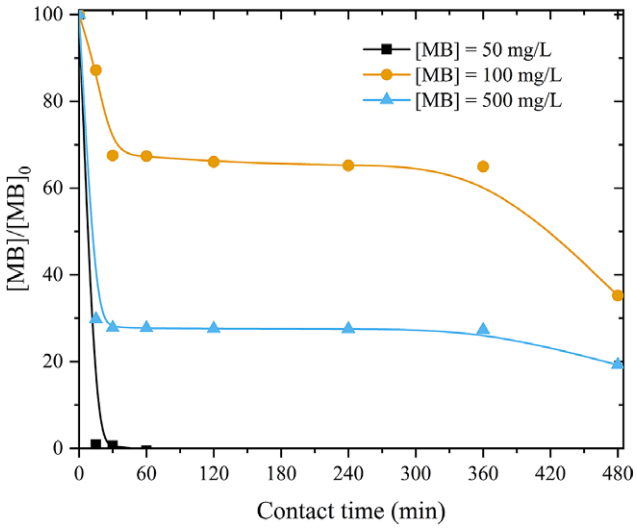

Figure 9. Effect of the initial concentration of MB on amount adsorbed by the Shymkent-TEAO clay. Conditions: $C_{adsorbent}$=2.5 g L^{-1}; $[MB]_0$=50, 100, and 500 mg L^{-1}; T=50°C; pH_0=3.0.

Effect of methylene blue concentration

As expected, the adsorption efficiency of MB on Shymkent-TEAO modified clay at various initial MB concentrations (Fig. 9) increased as the MB concentration decreased. The main active center for the Shymkent-TEAO sample is the nitrogen moiety from the TEAO molecule. Adsorption is governed by the free energy of adsorption of the surface, so the extent of adsorption depends on both the magnitude of the free energy and the amount of surface area available. As the clay developed here has a relatively small surface area (9 m^2 g^{-1}), the adsorption capacity is limited. Thus, the adsorbents prepared here would be most effective when applied in industrial wastewater streams in which the MB concentration is not too large, e.g. 10–50 mg L^{-1} (Yaseen and Scholz, 2019). This range of MB contamination is found widely, thus making Shymkent-TEAO suitable for MB clean-up, with the added advantage of enabling lower doses of adsorbent to be used than those for unmodified clay.

Conclusions

Clays (natural and modified) are inexpensive adsorbents that have been used successfully over recent decades in the adsorption of dyes from wastewater. The incorporation of a tertiary amine, TEAO, in the natural clay allowed a significant increase in the adsorption capacity of the clay, even if the textural properties were not improved. The reason ascribed to this phenomenon was the Lewis base character of the nitrogenated moiety. The presence of such an active center allowed a greater interaction of the adsorbent with MB. Due to its improved characteristics, Shymkent-TEAO was able to ensure the effective removal of MB from aqueous solutions. It was also demonstrated that the solution pH was not the key factor in the adsorption, specifically due to the presence of the Lewis

https://doi.org/10.1017/cmn.2024.34 Published online by Cambridge University Press

base active center. This feature opens future prospects for the development of economically viable adsorption-based technologies that can reduce the spread of MB in urban water cycles. However, further studies should include an assessment of environmental toxicity in real application scenarios in which several micro-pollutants are present in trace concentrations, and not just one pollutant in a concentration exceeding that observed in urban water cycles.

Supplementary material. The supplementary material for this article can be found at http://doi.org/10.1017/cmn.2024.34.

Data availability statement. Necessary data has been provided along with this manuscript.

Acknowledgements. None

Author contribution. Aizhan M. Serikbayeva: Conceptualization, Investigation, Formal analysis, Methodology, Visualization, Writing – original draft. Fernanda F. Roman: Investigation, Writing – Review and Editing. Helder T. Gomes: Funding acquisition, Project administration, Writing – Review & editing, Supervision. Marzhan S. Kalmakhanova: Writing – Review & Editing, Funding acquisition, Project administration, Supervision.

Financial support. This research was funded by the Science Committee of the Ministry of Education and Science of the Republic of Kazakhstan (grant no. AP13067715) and by Base Funding of CIMO (UIDB/00690/2020) through FEDER under Program PT2020.

Competing interest. The authors declare none.

References

Ahmadi, A., Foroutan, R., Esmaeili, H., & Tamjidi, S. (2020). The role of bentonite clay and bentonite clay@$MnFe_2O_4$ composite and their physico-chemical properties on the removal of Cr(III) and Cr(VI) from aqueous media. *Environmental Science and Pollution Research*, *27*, 14044–14057. https://doi.org/10.1007/s11356-020-07756-x

Ahmed, A., Chaker, Y., Belarbi, E.H., Abbas, O., Chotard, J.N., Abassi, H.B., Van Nhien, A.N., El Hadri, M., & Bresson, S. (2018). XRD and ATR/FTIR investigations of various montmorillonite clays modified by monocationic and dicationic imidazolium ionic liquids. *Journal of Molecular Structure*, *1173*, 653–664. https://doi.org/10.1016/j.molstruc.2018.07.039

Ali, N., Ali, F., Ullah, I., Ali, Z., Duclaux, L., Reinert, L., Lévêque, J.M., Farooq, A., Bilal, M., & Ahmad, I. (2020). Organically modified micron-sized vermiculite and silica for efficient removal of Alizarin Red S dye pollutant from aqueous solution. *Environmental Technology & Innovation*, *19*, 101001. https://doi.org/10.1016/j.eti.2020.101001

Auerbach, S.M., Carrado, K.A., & Dutta, P.K. (eds) (2004). *Handbook of Layered Materials*. CRC Press. https://doi.org/10.1201/9780203021354

Baimuratova, Zh.A., Kalmakhanova, M.S., Shynazbekova, Sh.S., Kybyraeva, N. S., Díaz de Tuesta, J.L., & Gomes, H.T. (2022). $MnFe_2O_4$/Zhetisay composite as a novel magnetic material for adsorption of Ni(II). *News of the Academy of Sciences of the Republic of Kazakhstan. Series of Geology and Technical Sciences*, *2*, 58–72. https://doi.org/10.32014/2022.2518-170x.160

Baimuratova, Z., Ermekov, S., Silva, A, Gomes, H., & Kalmakhanova, M. (2024). New magnetic clays $MnFe_2O_4$/Shymkent for removal of heavy metals from wastewater. *E3S Web of Conferences*, *474*, 01034. https://doi.org/10.1051/e3sconf/202447401034

Bardestani, R., Patience, G.S., & Kaliaguine, S. (2019). Experimental methods in chemical engineering: specific surface area and pore size distribution measurements – BET, BJH, and DFT. *Canadian Journal of Chemical Engineering*, *97*, 2781–2791. https://doi.org/10.1002/cjce.23632

Brunauer, S., Deming, L.S., Deming, W.E., & Teller, E. (1940). On a theory of the van der Waals adsorption of gases. *Journal of the American Chemical Society*, *62*, 1723–1732. https://doi.org/10.1021/JA01864A025

Caglar, B. (2012). Structural characterization of kaolinite-nicotinamide intercalation composite. *Journal of Molecular Structure*, *1020*, 48–55. https://doi.org/10.1016/j.molstruc.2012.03.061

Cheng, H., Liu, Q., Zhang, J., Yang, J., & Frost, R.L.J. (2010). The thermal behavior of kaolinite intercalation complexes – a review. *Colloids and Surfaces A*, *348*, 355. https://doi.org/10.1016/j.tca.2012.04.005

Diaz De Tuesta, J. L., Roman, F.F., Marques, V.C., Silva, A.S., Silva, A.P.F., Bosco, T.C., Shinibekova, A.A., Aknur, S., Kalmakhanova, M.S., Massalimova, B.K., Arrobas, M., Silva, A.M.T., & Gomes, H.T. (2022). Performance and modeling of Ni(II) adsorption from low concentrated wastewater on carbon microspheres prepared from tangerine peels by $FeCl_3$-assisted hydrothermal carbonization. *Journal of Environmental Chemical Engineering*, *10*, 108143. https://doi.org/10.1016/j.jece.2022.108143

Diaz de Tuesta, J.L., Silva, A.M.T., Faria, J.L., & Gomes, H.T. (2018). Removal of Sudan IV from a simulated biphasic oily wastewater by using lipophilic carbon adsorbents. *Chemical Engineering Journal*, *347*, 963–971. https://doi.org/10.1016/j.cej.2018.04.105

Diaz de Tuesta, J.L., Saviotti, M.C., Roman, F.F., Pantuzza, G.F., Sartori, H.J.F., Shinibekova, A., Kalmakhanova, M.S., Massalimova, B.K., Pietrobelli, J.M.T. A., Lenzi, G.G., & Gomes, H.T. (2021) Assisted hydrothermal carbonization of agroindustrial byproducts as an effective step in the production of activated carbon catalysts for wet peroxide oxidation of micro-pollutants. *Journal of Environmental Chemical Engineering*, *9*, 105004. https://doi.org/10.1016/j.jece.2020.105004

Elkhalifah, A.E.I., Bustam, M.A., Azmi, M.S., & Murugesan, T. (2014a). Carbon dioxide retention on bentonite clay adsorbents modified by mono-, di- and triethanolamine compounds. *Advanced Materials Research*, *917*, 115–122. https://doi.org/10.4028/www.scientific.net/amr.917.115

Elkhalifah, A.E.I., Bustam, M.A., Mohd Shariff, A., Ullah, S., Shimekit, B., & Riaz, N. (2014b). Effects of intercalated mono-, di- and triethanolammonium cations on the structural and surface characteristics of sodium form of bentonite. *Applied Mechanics and Materials*, *625*, 98–101. https://doi.org/10.4028/www.scientific.net/amm.625.98

Elmoubarki, R., Mahjoubi, F.Z., Tounsadi, H., Moustadraf, J., Abdennouri, M., Zouhri, A., Albani, A.E., & Barka, N. (2015). Adsorption of textile dyes on raw and decanted Moroccan clays: kinetics, equilibrium, and thermodynamics. *Water Resources and Industry*, *9*, 16–29. https://doi.org/10.1016/j.wri.2014.11.001

Esvandi, Z., Foroutan, R., Peighambardoust, S.J., Akbari, A., & Ramavandi, B. (2020). Uptake of anionic and cationic dyes from water using natural clay and clay/starch/$MnFe_2O_4$ magnetic nanocomposite. *Surfaces and Interfaces*, *21*, 100754. https://doi.org/10.1016/j.surfin.2020.100754

Fan, H., Zhou, L., Jiang, X., Huang, Q., & Lang, W. (2014). Adsorption of Cu^{2+} and methylene blue on dodecyl sulfobetaine surfactant-modified montmorillonite. *Applied Clay Science*, *95*, 150–158. https://doi.org/10.1016/j.clay.2014.04.001

Ferreira, B.F., Ciuffi, K.J., Nassar, E.J., Vicente, M.A., Trujillano, R., Rives, V., & Faria, E.H. (2017). Kaolinite-polymer compounds by grafting of 2-hydroxyethyl methacrylate and 3-(trimethoxysilyl)propyl methacrylate. *Applied Clay Science*, *146*, 526–534. https://doi.org/10.1016/j.clay.2017.07.009

Godarziani, H., Ramezanipour Penchah, H., & Ghaemi, A. (2022). Triethanolamine-modified montmorillonite clay as a new adsorbent for CO_2 capture: characterization, adsorption, and RSM modeling. *Journal of the Chinese Chemical Society*, *69*, 1981–1996. https://doi.org/10.1002/jccs.202200395

Gregg, S., & Sing, K. (1982). *Adsorption, Surface Area, and Porosity*. New York: Academic Press.

Guerra, D.L., Airoldi, C., & Sousa, K.S. (2008). Adsorption and thermodynamic studies of Cu(II) and Zn(II) on organofunctionalized-kaolinite. *Applied Surface Science*, *254*, 5157. https://doi.org/10.1016/j.apsusc.2008.02.017

Haleem, A., Anum, S., Chen, S.-Q., & Nazar, M. (2023). A comprehensive review on adsorption, photocatalytic and chemical degradation of dyes and nitro-compounds over different kinds of porous and composite materials. *Molecules*, *28*, 1081. https://doi.org/10.3390/molecules28031081

Jawad, A.H., Saber, S.E.M., Abdulhameed, A.S., Farhan, A.M., ALOthman, Z.A., & Wilson, L.D. (2023). Characterization and applicability of the natural Iraqi bentonite clay for toxic cationic dye removal: adsorption kinetic and isotherm

study. *Journal of King Saud University – Science*, *35*, 102630. https://doi.org/10.1016/j.jksus.2023.102630

Junior, H.B., da Silva, E., Saltarelli, M., Crispim, D., Nassar, E.J., Trujillano, R., Rives, V., Vicente, M.A., Gil, A., Korili, S.A., de Faria, E.H., & Ciuffi, K.J. (2020). Inorganic–organic hybrids based on sepiolite as efficient adsorbents of caffeine and glyphosate pollutants. *Applied Surface Science Advances*, *1*, 100025. https://doi.org/10.1016/j.apsadv.2020.100025

Kalmakhanova, M.S., Diaz de Tuesta, J.L., Malakar, A., Gomes, H.T., & Snow, D. D. (2023). Wastewater treatment in central asia: treatment alternatives for safewater reuse. *Sustainability*, *15*, 14949. https://doi.org/10.3390/su152014949

Karimi, M., Diaz de Tuesta, J.L., Gonçalves, C.N.d.P., Gomes, H.T., Rodrigues, A.E., & Silva, J.A.C. (2020). Compost from municipal solid wastes as a source of biochar for CO_2 capture. *Chemical Engineering & Technology*, *43*, 1336–1349. https://doi.org/10.1002/ceat.201900108

Kausar A., & Bhatti H.N. (2013). Adsorptive removal of uranium from wastewater: a review. *Journal of Chemical Society of Pakistan*, *35*, 1041–1052. https://doi.org/10.2139/ssrn.4524308

Khan, M.I., Khan, H.U., Azizli, K., Sufian, S., Man, Z., Siyal, A.A., Muhammad, N., & Faiz ur Rehman, M. (2017). The pyrolysis kinetics of the conversion of Malaysian kaolin to metakaolin. *Applied Clay Science*, *146*, 152–161. https://doi.org/10.1016/j.clay.2017.05.017

Koteja, A., & Matusik, J. (2015). Di- and triethanolamine grafted kaolinites of different structural order as adsorbents of heavy metals. *Journal of Colloid and Interface Science*, *455*, 83–92. https://doi.org/10.1016/j.jcis.2015.05.027

Lagaly, G., Ogawa, M., & Dékány, I. (2013). Chapter 10.3 – Clay mineral–organic interactions. In *Handbook of Clay Science* (eds) Bergaya F., & Lagaly G., pp. 435–505 Elsevier.

Letaief, S., & Detellier, C. (2011). Application of thermal analysis for the characterization of intercalated and grafted organo-kaolinite nanohybrid materials. Journal of Thermal Analysis and Calorim*etry*, *104*, 831–839. https://doi.org/10.1007/s10973-010-1269-8

Lorentz, B., Shanahan, N., Stetsko, Y.P., & Zayed, A. (2018). Characterization of Florida kaolin clays using multiple-technique approach. *Applied Clay Science*, *161*, 326–333. https://doi.org/10.1016/j.clay.2018.05.001

Lowell, S., Shields, J.E., Thomas, M.A., & Thommes, M. (2004). Surface area analysis from the Langmuir and BET theories. In *Characterization of Porous Solids and Powders: Surface Area, Pore Size and Density. Particle Technology Series*, vol. *16*. Springer, Dordrecht. https://doi.org/10.1007/978-1-4020-2303-3_5

Machado, G.S., Groszewicz, P.B., Castro, K.A.D.F., Wypych, F.S., & Nakagaki, J. (2012). Catalysts for heterogeneous oxidation reaction based on metalloporphyrins immobilized on kaolinite modified with triethanolamine. *Journal of Colloid and Interface Science*, *374*, 278. https://doi.org/10.1016/j.jcis.2012.02.014

Matusik, J., & Wścisło, A. (2014). Enhanced heavy metal adsorption on functionalized nanotubular halloysite interlayer grafted with aminoalcohols. *Applied Clay Science*, *100*, 50–59. https://doi.org/10.1016/j.clay.2014.06.034

Mnasri-Ghnimi, S., & Frini-Srasra, N. (2019). Removal of heavy metals from aqueous solutions by adsorption using single and mixed pillared clays. *Applied Clay Science*, *179*, 105151, https://doi.org/10.1016/j.clay.2019.105151

Mukhopadhyay, R., Sarkar, B., Palansooriya, K.N., Dar, J.Y., Bolan, N.S., Parikh, S.J., Sonne, C., & Ok, Y.S. (2021). Natural and engineered clays and clay minerals for the removal of poly- and perfluoroalkyl substances from water: state-of-the-art and future perspectives. *Advances in Colloid and Interface Science*, *297*, 102537. https://doi.org/10.1016/j.cis.2021.102537

Mundkur, N., Khan, A.S., Khamis, M.I., Ibrahim, T.H., & Nancarrow, P. (2022). Synthesis and characterization of clay-based adsorbents modified with alginate, surfactants, and nanoparticles for methylene blue removal. *Environmental Nanotechnology, Monitoring & Management*, *17*, 100644). https://doi.org/10.1016/j.enmm.2022.100644

Nadeem, R., Manzoor, Q., Iqbal, M., & Nisar, J. (2016). Biosorption of Pb(II) onto immobilized and native *Mangifera indica* waste biomass. *Journal of Industrial and Engineering Chemistry*, *35*, 185–194. https://doi.org/10.1016/j.jiec.2015.12.030

Naeem, H., Bhatti, H.N., Sadaf, S., & Iqbal, M. (2017). Uranium remediation using modified *Vigna radiata* waste biomass. *Applied Radiation and Isotopes*, *123*, 94–101. https://doi.org/10.1016/j.apradiso.2017.02.027

Qi, J., Yu, J., Shah, K.J., Shah, D.D., & You, Z. (2023). Applicability of clay/organic clay to environmental pollutants: green way – an overview. *Applied Science*, *13*, 9395. https://doi.org/10.3390/app13169395

Rahmani, S., Zeynizadeh, B., & Karami, S. (2020). Removal of cationic methylene blue dye using magnetic and anionic-cationic modified montmorillonite: kinetic, isotherm and thermodynamic studies. *Applied Clay Science*, *184*, 105391. https://doi.org/10.1016/j.clay.2019.105391

Rashid, A., Bhatti, H.N., Iqbal, M., & Noreen, S. (2016). Fungal biomass composite with bentonite efficiency for nickel and zinc adsorption: a mechanistic study. *Ecological Engineering*, *91*, 459–471. https://doi.org/10.1016/j.ecoleng.2016.03.014

Reimbaeva, S.M., Massalimova, B.K., & Kalmakhanova, M.S. (2020). New pillared clays prepared from different deposits of Kazakhstan. *Materials Today: Proceedings*, *31*, 607–610. https://doi.org/10.1016/j.matpr.2020.07.532

Ruiz-Rosas, R., García-Mateos, F.J., Gutiérrez, M.C., Rodríguez-Mirasol, J., & Cordero, T. (2019). About the role of porosity and surface chemistry of phosphorus-containing activated carbons in the removal of micropollutants. *Frontiers in Materials*, *6*, 134. https://doi.org/10.3389/fmats.2019.00134

Saeed, M., Munir, M., Nafees, M., Shah, S.S.A., Ullah, H., & Waseem, A. (2020). Synthesis, characterization and applications of silylation based grafted bentonites for the removal of Sudan dyes: isothermal, kinetic and thermodynamic studies. *Microporous and Mesoporous Materials*, *291*, 109697. https://doi.org/10.1016/j.micromeso.2019.109697

Serikbayeva, A.M., Kalmakhanova, M.S., Massalimova, B.K., Zharlykapova, R.B., & Bazarbaev, H. (2021). Preparation and physico-chemical characterization of organic modified clays with grafted organoalkoxides. *News of the Academy of Sciences of the Republic of Kazakhstan, Series Chemistry and Technology*, *5–6*, 61–68. https://doi.org/10.32014/2021.2518-1491.78.

Sharma, P., Borah, D.J., Das, P., & Das, M.R. (2015). Cationic and anionic dye removal from aqueous solution using montmorillonite clay: evaluation of adsorption parameters and mechanism. *Desalination and Water Treatment*, *57*, 8372–8388. https://doi.org/10.1080/19443994.2015.1021844

Shoukat, S., Bhatti, H.N., Iqbal, M., & Noreen, S. (2017). Mango stone biocomposite preparation and application for crystal violet adsorption: a mechanistic study. *Microporous and Mesoporous Materials*, *239*, 180–189. https://doi.org/10.1016/j.micromeso.2016.10.004

Silva, A.S., Kalmakhanova, M.S., Massalimova, B.K., Sgorlon, J.G., Diaz de Tuesta, J.L., & Gomes, H.T. (2019). Wet peroxide oxidation of paracetamol using acid activated and Fe/Co-pillared clay catalysts prepared from natural clays. *Catalysts*, *9*, 705. https://doi.org/10.3390/catal9090705

Sing, K., Everett, D., Haul, R., Moscou, L., Pierotti, R., Rouquerol, J., & Siemieniewska, T. (1985). Physical and biophysical chemistry division commission on colloid and surface chemistry including catalysis. *Pure and Applied Chemistry*, *57*, 603–619.

Souhassou, H., Khallouk, K., El Khalfaouy, R., El Gaidoumi, A., Nahali, L., Fahoul, Y., Tanji, K., & Kherbeche, A. (2023). Optimization of a binary dye mixture adsorption by Moroccan clay using the Box-Behnken experimental design. *Chemistry Africa*, *6*, 2011–2027. https://doi.org/10.1007/s42250-023-00608-4

Suchithra, P.S., Vazhayal, L, Mohamed, A.P., & Ananthakumar, S. (2012). Mesoporous organic–inorganic hybrid aerogels through ultrasonic assisted sol–gel intercalation of silica–PEG in bentonite for effective removal of dyes, volatile organic pollutants and petroleum products from aqueous solution. *Chemical Engineering Journal*, *200–202*, 589–600. https://doi.org/10.1016/j.cej.2012.06.083

Sun, D., Li, B., Li, Y., Yu, C., Zhang, B., & Fei, H. (2011). Characterization of exfoliated/delamination kaolinite. *Materials Research Bulletin*, *46*, 101. https://doi.org/10.1016/j.materresbull.2010.09.031

Tahir, M.A., Bhatti, H.N., & Iqbal, M. (2016a). Solar red and brittle blue direct dyes adsorption onto Eucalyptus angophoroides bark: equilibrium, kinetics, and thermodynamic studies. *Journal of Environmental Chemical Engineering*, *4*, 2431–2439. https://doi.org/10.1016/j.jece.2016.04.020

Tahir, N., Bhatti, H.N., Iqbal, M., & Noreen, S. (2016b). Biopolymers composites with peanut hull waste biomass and application for crystal violet adsorption. *International Journal of Biological Macromolecules*, *94*, 210–220. https://doi.org/10.1016/j.ijbiomac.2016.10.013

Tahir, M., Iqbal, M., Abbas, M., Tahir, M., Nazir, A., Iqbal, D.N., Kanwal, Q., Hassan, F., & Younas, U. (2017). Comparative study of heavy metals

https://doi.org/10.1017/cmn.2024.34 Published online by Cambridge University Press

distribution in soil, forage, blood, and milk. *Acta Ecologica Sinica*, *37*, 207–212. https://doi.org/10.1016/j.chnaes.2016.10.007

Teixeira, R.A., Lima, E.C., Benetti, A.D., Naushad, M., Thue, P.S., Mello, B.L., Reis, G.S., Rabiee, N., Franco, D., & Seliem, M.K. (2023). Employ a Clay@TMSPDETA hybrid material as an adsorbent to remove textile dyes from wastewater effluents. *Environmental Science & Pollution Research*, *30*, 86010–86024. https://doi.org/10.1007/s11356-023-28568-9

Tkaczyk, A., Mitrowska, K., & Posyniak, A. (2020). Synthetic organic dyes as contaminants of the aquatic environment and their implications for ecosystems: a review. *Science of the Total Environment*, *717*, 137222. https://doi.org/10.1016/j.scitotenv.2020.137222

Tripathi, M., Singh, S., Pathak, S., Kasaudhan, J., Mishra, A., Bala, S., Garg, D., Singh, R., Singh, P., Singh, P.K., Shukla, A.K., & Pathak, N. (2023). Recent strategies for the remediation of textile dyes from wastewater: a systematic review. *Toxics*, *11*, 940. https://doi.org/10.3390/toxics11110940

Yang, Q., Wang, B., Chen, Y., Xie, Y., & Li, J. (2019). An anionic In(III)-based metal-organic framework with Lewis basic sites for the selective adsorption and separation of organic cationic dyes. *Chinese Chemical Letters*, *30*, 234–238. https://doi.org/10.1016/j.cclet.2018.03.023

Yaseen, D.A., & Scholz, M. (2019). Textile dye wastewater characteristics and constituents of synthetic effluents: a critical review. *International Journal of Environmental Science and Technology*, *16*, 1193–1226. https://doi.org/10.1007/s13762-018-2130-z

Yuan, P, Southon, P.D., Liu, Z., Green, M.E.R., Hook, J.M., Antill, S.J., & Kepert, C.J. (2008). Functionalization of halloysite clay nanotubes by grafting with aminopropyl triethoxysilane. *Journal of Physical Chemistry C*, *112*, 15742–15751. https://doi.org/10.1021/jp805657t

Zakharova, M.V., Masoumifard, N., Hu, Y., Han, J., Kleitz, F., & Fontaine, F.-G. (2018). Designed synthesis of mesoporous solid-supported Lewis acid–base pairs and their CO_2 adsorption behaviors. *ACS Applied Materials & Interfaces*, *10*, 13199–13210. https://doi.org/10.1021/acsami.8b00640

Zhang, T., Wang, W., Zhao, Y., Bai, H., Wen, T., Kang, S., Song, G., Song, S., & Komarneni, S. (2021). Removal of heavy metals and dyes by clay-based adsorbents: from natural clays to 1D and 2D nano-composites. *Chemical Engineering Journal*, *420*, 127574. https://doi.org/10.1016/j.cej.2020.127574

https://doi.org/10.1017/cmn.2024.34 Published online by Cambridge University Press